Int. J. Heat Mass Transfer. Vol. 28, No. 3, pp. 641–651, 1985
Printed in Great Britain

0017-9310/85 $3.00 + 0.00

Convective–radiative heat transfer from a horizontal finned tube with sidewall or sidewall/floor interactions

E. M. SPARROW and M. A. ANSARI
Department of Mechanical Engineering, University of Minnesota, Minneapolis, MN 55455, U.S.A.

(*Received* 27 *June* 1984 *and in final form* 10 *September* 1984)

Abstract—Experiments were performed to determine how the heat transfer from a horizontal finned tube responds to the presence of a sidewall or of a sidewall/floor system. The clearances between the fin tips and the sidewall and between the fin tips and the floor were varied parametrically and, for each configuration, heat transfer results were obtained over a 25-fold range of the tube-to-ambient temperature difference. Measurements were also made for the finned tube situated in free space (i.e. far from any walls), and these results displayed highly enhanced heat transfer (by a factor of 4–8 times) compared to a corresponding unfinned tube. The presence of a sidewall had only a moderate effect on the finned-tube heat transfer, whereas the sidewall/floor system caused greater changes. The extreme reduction in heat transfer due to the latter was about 40%, but reductions in the 10–20% range are more realistic for practical operating conditions. In percentage terms, the presence of the wall(s) had less effect at large temperature differences than at small temperature differences. Measured temperatures at the fin tips, on the sidewall, and on the floor are also presented.

INTRODUCTION

HORIZONTAL finned tubes cooled by natural convection and radiation are used extensively in space heating applications. In typical installations, the finned tube is situated in close proximity either to a sidewall or to the intersection of a sidewall and a floor. A variety of interactions may occur between these walls and the finned tube, encompassing all modes of heat transfer. These interactions will affect the heat transfer performance of a finned tube to an extent which depends on the distance between the tube and the wall(s). It is the objective of the present research to determine the heat transfer characteristics of a horizontal finned tube situated in air in the presence of either a sidewall or of a sidewall/floor corner.

It is relevant to identify the most significant of the finned-tube/wall interactions. In practice, the wall and/or the floor situated adjacent to a heated finned tube are made of low conductivity materials, so that they are approximately adiabatic. Therefore, due to the absorption of radiation emitted by the heated finned tube, the surfaces of the wall(s) attain temperatures that are elevated above that of the ambient (the surfaces usually have high emissivities and absorptivities). This temperature elevation is a key factor in the thermal interaction between the tube and the wall(s).

In particular, the net radiative heat loss from the finned tube is diminished because it absorbs radiation emitted by the wall(s). Also, owing to their elevated temperature, the wall(s) impart a buoyancy to the air which is additional to the buoyancy created by the finned tube itself. The additional buoyancy tends to enhance the convective heat transfer from the finned tube, thereby working oppositely to the aforementioned radiation effect.

Another significant effect of the presence of the walls, especially of the sidewall/floor system, is the blockage of the adjacent portion of the finned tube, making it difficult for the air to penetrate there. The blockage tends to reduce the convective heat transfer. When the fin tips are very close to the walls, direct heat conduction may occur between the tips and the walls. However, since the walls are nearly adiabatic and the tip surface area is small, the conduction is a minor effect.

The foregoing discussion of the finned-tube/wall interactions points up the interdependence of radiation and natural convection. The tight intermingling of the two modes is also present in the finned-tube heat transfer, even when there are no nearby walls. Because the surfaces of the finned tube are usually painted and because the cavity-like interfin spaces give rise to an apparent emissivity which exceeds the actual emissivity, the radiation heat transfer tends to be comparable to that by natural convection.

The subdivision of the finned-tube heat transfer into convective and radiative components is difficult because of the complexity and interactive nature of the system. Such a subdivision would necessarily involve a highly approximate analysis, yielding results of uncertain accuracy. Furthermore, it would have little merit from the standpoint of practice, since the all-modes heat transfer is needed for design. In view of this, the results to be presented here are for the all-modes heat transfer.

The finned-tube apparatus used in the research was especially fabricated to avoid thermal contact resistance between the fins and the tube and to be free of

NOMENCLATURE

A	total heat transfer surface area of finned tube
A_{tube}	heat transfer surface area of unfinned tube
D	tube diameter
g	acceleration of gravity
h_{tube}	convective heat transfer coefficient for unfinned tube
h^*	convective–radiative heat transfer coefficient for no-walls case
k	thermal conductivity
L	side length of square fins
L_h	clearance between sidewall and fin tips
L_v	clearance between floor and fin tips
Nu^*	Nusselt number for no-walls case, h^*S/k
Pr	Prandtl number
Q	finned-tube heat transfer rate
Q^*	value of Q for no-walls case
Q_{tube}	heat transfer rate for unfinned tube
Ra	Rayleigh number, $[g\beta(T_w - T_\infty)S^3/\nu^2]Pr$
S	interfin spacing
T_f	temperature at floor
T_{sw}	temperature at sidewall
T_{tip}	fin tip temperature
T_w	tube wall temperature
T_∞	ambient temperature
t	fin thickness
X	coordinate along floor (Fig. 10)
Y	coordinate along sidewall (Fig. 10).

Greek symbols

β	coefficient of thermal expansion
ε	emissivity
ν	kinematic viscosity
σ	Stefan–Boltzmann constant.

extraneous heat losses and end effects. The apparatus dimensions were chosen to conform to the dimensions commonly encountered in actual finned-tube heaters, and the radiation surface properties of the finned tube and the wall(s) also corresponded to those of practice.

Three distinct sets of experiments were performed. First, to provide baseline information, heat transfer data were obtained for the horizontal finned tube situated in free space (i.e. without a sidewall or floor). The second set of experiments dealt with the interaction of the finned tube with a sidewall, while in the third set, the interaction between the finned tube and an intersecting sidewall and floor was investigated. The clearance gap between the sidewall and the adjacent edges of the fins was varied from about 2 to 100% of the fin side dimension, while the gap between the floor and the fin edges ranged from about 2% of the fin side dimension to infinity. For each geometrical configuration, the Rayleigh number, which represents the dimensionless temperature difference between the tube and ambient, was varied by a factor of 25.

To provide a direct measure of the effects of the finned-tube/wall interactions, the heat transfer results for the interactive configurations are presented as a ratio with respect to the results for the finned tube in free space. In addition to heat transfer results, fin tip temperatures and temperature distributions along the sidewall and the floor are also presented.

A survey of the literature indicated that there was virtually no prior work on heat transfer from finned tubes interacting with adjacent walls. The only relevant publication [1] is a design-oriented collection of formulas and graphs for computing heat transfer rates. No actual experimental data are presented nor are the underlying experiments described. The heat transfer results apply to the single temperature difference of 150°F between steam condensing inside the tube and the ambient. Furthermore, the range of the investigated gaps between the fin tips and the adjacent walls was limited, especially in the case of the floor.

EXPERIMENTAL

The finned tube

As noted earlier, a specially designed and fabricated finned tube was employed in the experiments to ensure the absence of fin-tube contact resistance, extraneous temperature nonuniformities and heat losses, and end effects. The main features of the apparatus will now be described, with additional details available in [2].

The underlying design concept was to create a finned tube which, after fabrication, was a single, continuous unit. To this end, the finned tube was synthesized by succesively stacking copper spacer rings between square copper fins, with the result depicted in the longitudinal sectional view of Fig. 1. The actual assembly operations were performed in a furnace, with

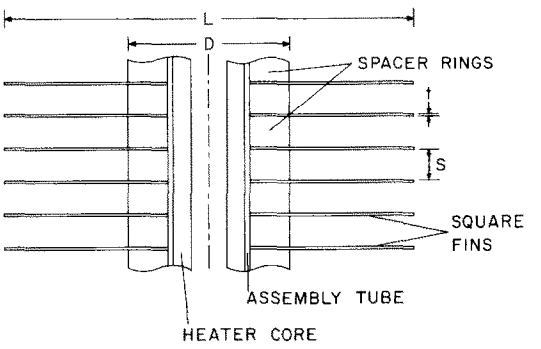

FIG. 1. Longitudinal sectional view of the finned tube.

solder introduced at all the contacting faces of the rings and the fins. To ensure perfect contact at these faces and to eliminate excess solder, a ram was periodically tightened down on the stack at various stages during its assembly. As seen in the figure, the radial width of the spacer rings was chosen to provide an amply large area of contact with the faces of the fins.

After completion of the assembly, the spacer rings formed a thick-walled copper tube, with the fins being, in effect, integral with the tube. The outer circumferential faces of the rings served as the surface of the tube exposed to the airflow.

In addition to the finned tube proper, Fig. 1 also shows the assembly tube (made of brass) on which the stacking of the rings and fins was performed. During that operation, the assembly tube was incorporated into an alignment fixture which centered the rings and fins and which aligned the edges of the fins.

A specially fabricated brass heater core, wound to provide both circumferentially and axially uniform heating, was inserted into the bore of the tube subsequent to the completion of the assembly. Copper oxide cement was used to ensure good thermal contact. The hollow bore of the heater core served as a passageway through which thermocouple lead wires were conveyed from the tube wall to the outside.

The fins were cut from a sheet of 0.0508-cm thick, oxygen-free copper. Each fin was precisely machined to a 8.128 × 8.128 cm square, with a concentric center hole of 1.595 cm diameter. Before the assembly operations, the portion of each fin to be exposed to the airflow was spray painted with a high-temperature black paint, but no paint was permitted on that part of the fin face that would contact the face of a spacer ring.

The spacer rings were fabricated from oxygen-free copper rod stock, turned to the desired outside diameter of 3.188 cm and bored to an inner diameter of 1.595 cm. Each spacer ring had a finished axial length of 0.584 cm, which also served as the interfin spacing. The outer circumferential face of each ring was spray painted with the same high-temperature black paint used for the surfaces of the fins, but the other surfaces of the rings were left unpainted.

The emissivity of the black-painted surfaces was measured with a Gier–Dunkle heated-cavity reflectometer to be 0.87, a value typical of paints in general.

The key dimensions of the finned tube, expressed in the notation of Fig. 1, are

$$L = 8.128 \text{ cm}, \quad D = 3.188 \text{ cm}, \quad S = 0.584 \text{ cm},$$

$$t = 0.0508 \text{ cm}.$$

Note that the axial pitch $(S+t)$ is 0.635 cm, which corresponds to four fins per inch—a pitch common to practical finned-tube heaters. A total of 48 rings and 49 fins were employed, which yielded an overall length of the finned tube of 30.48 cm.

To avoid extraneous conduction losses which would have occurred with a conventional support system, the finned tube was suspended by nylon line (0.06-cm diameter). Extraneous convection losses from the outboard face of the first and last fin of the array were virtually eliminated by a block of resilient R11 fiberglass affixed to the respective face by double-sided tape.

The finned tube was equipped with eleven thermocouples (0.0254-cm diameter, Teflon-coated, chromel and constantan wire), deployed so as to provide information about the axial and circumferential distributions of the wall temperature. Typically, the deviation of any one thermocouple reading from the arithmetic mean did not exceed 0.25% of the wall-to-ambient temperature difference. The thermocouple junctions were situated 0.0254 cm from the exposed surface of the spacer rings. Installation of the thermocouples was performed subsequent to the assembly of the finned tube, using the special procedure described in [2].

Thermocouples were also installed at the tips of representative fins to provide an indication of the fin efficiency (i.e. the radial temperature drop in the fin) and of the circumferential temperature variation. The thermocouple junctions were affixed by solder at the centers of the top, side and bottom edges of the respective fins. To minimize temperature measurement errors, small diameter wire (0.00762 cm, Teflon-coated chromel and constantan) was used and the leads were laid along the edges of the fins.

Other features of the experiments

The positioning of the finned tube with respect to the sidewall and to the sidewall/floor system is illustrated in Fig. 2. The separation distance between the sidewall and the tips of the adjacent fins is denoted by L_h (h ~ horizontal) while the floor–fin tip distance is denoted by L_v (v ~ vertical). For the sidewall/floor system, L_h and L_v were independently adjustable. The variations of L_h and L_v were accomplished by moving the sidewall and the floor respectively, with the finned tube remaining stationary.

The sidewall and the floor were of similar construction. The basic structural element was a 1.27-cm thick plywood sheet to whose rear face angle iron braces were fastened to ensure flatness. The front face of the plywood was carefully sanded and then covered with a 0.006-cm thick sheet of self-adhering, plasticized contact paper in order to present a hydrodynamically smooth surface to the airflow. Contact paper was also used to seal the corner at the intersection of the sidewall and the floor. The high emissivity of the contact paper (measured to be 0.855) is typical of surfaces that are in close proximity to heated finned tubes. An insulation pack consisting of 5.08 cm of polystyrene and 8.89 cm of fiberglass, affixed to the rear of the plywood, served to block heat flow through the sidewall and the floor.

The face dimensions of the sidewall were 63.50 × 78.74 cm (height × width), while those of the floor were 91.44 × 78.74 cm (length × width). The sidewall and the floor were sufficiently large so that from the standpoint

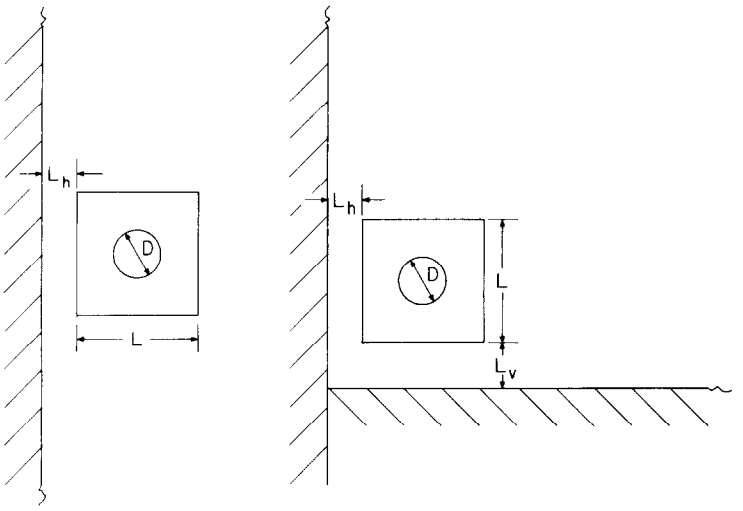

FIG. 2. Positioning of the finned tube with respect to the sidewall and to the sidewall/floor system.

of the participating heat transfer processes, they appeared to be infinite in extent.

Thermocouples were installed to measure surface temperature distributions on the sidewall and the floor. The thermocouple locations will be evident from the results to be presented later.

The experiments were performed in a windowless, interior laboratory room situated in a temperature-controlled building. Room air currents were minimized by sealing off the ductwork, by blocking the door with a 10-cm thick slab of polystyrene, and by placing fiberglass batts on the floor. The instrumentation and the power supply were located in a service corridor situated adjacent to the laboratory. The laboratory was neither entered nor illuminated during the course of a data run as well as during a period prior to the run. Data were not collected until at least 6 h after the initiation of heating.

In addition to the temperature measurements mentioned earlier, the air temperature in the neighborhood of the finned tube was measured with a rake of four shielded thermocouples. Power was provided by a regulated AC supply, constant to 0.03% during a data run. During the course of the research, the power was varied so as to yield a variation of the temperature difference between the tube wall and ambient from 2.2 to 83.3°C (4 to 150°F).

DATA REDUCTION AND PARAMETERIZATION

The primary objective of this investigation is to determine how the rate of heat transfer from a horizontal finned tube is affected by the presence of a sidewall or a sidewall/floor system. This information will be reported via the ratio Q/Q^*. The quantity Q denotes the finned-tube heat transfer rate in the presence of the walls, while Q^* is the heat transfer rate for the same finned tube situated in free space (i.e. far from all walls). Q and Q^* correspond to the same values of the tube wall temperature T_w, of the ambient air temperature T_∞, and of the ambient pressure. The departure of Q/Q^* from one provides a direct measure of the presence of the wall(s), with $Q/Q^* < 1$ indicating a wall-related heat transfer reduction and $Q/Q^* > 1$ indicating a heat transfer increase.

Owing to the suppression of extraneous heat losses, the finned-tube heat transfer rate was obtained directly from the electric power input. To supplement the experiments which involved either a sidewall or a sidewall/floor system (and which yielded Q), a set of experiments was performed without a sidewall or floor in order to determine the values of Q^* needed to form the Q/Q^* ratio.

The Q/Q^* results will be presented as a function of three independent parameters. The separation distance between the sidewall and the adjacent fin tips will be expressed in dimensionless form as L_h/L, while the distance between the floor and the adjacent tips is represented by L_v/L. For each configuration defined by L_h/L and L_v/L, the temperature difference $(T_w - T_\infty)$ was varied parametrically. Since T_∞ was virtually constant throughout the entire investigation (23 ± 1°C), the temperature difference also serves as a measure of the tube wall temperature T_w. A dimensionless version of the temperature difference will be expressed via the Rayleigh number

$$Ra = [g\beta(T_w - T_\infty)S^3/\nu^2]Pr \qquad (1)$$

where the interfin spacing S (Fig. 1) has been used as the characteristic length. The thermophysical properties were evaluated at a reference temperature $\frac{1}{2}(T_w + T_\infty)$, except that $\beta = 1/T_\infty$ (absolute temperature).

The radiative contribution to the heat transfer is fixed by the emissivities of the participating surfaces and their geometry. The emissivity values of the present

apparatus, 0.87 for the fin and tube surfaces and 0.855 for the wall(s), are in the practical range. Furthermore, because of the cavity effect (the interfin spaces may be regarded as partially closed cavities), the radiative transfer should be insensitive to small deviations of the fin and tube emissivity from that of the present apparatus.

To complement the Q/Q^* ratios, the Q^* results are reported via the Nusselt number Nu^*

$$Nu^* = h^*S/k, \quad h^* = Q^*/A(T_w - T_\infty) \tag{2}$$

in which A is the total heat transfer surface area. The Q/Q^* ratio can also serve as a Nu/Nu^* ratio, if $h = Q/A(T_w - T_\infty)$ and $Nu = hS/k$.

In addition to the heat transfer results, representative temperature data are presented for the fin tips, the sidewall, and the floor. These results are conveyed by the ratios

$$(T_{tip} - T_\infty)/(T_w - T_\infty), \quad (T_{sw} - T_\infty)/(T_w - T_\infty), \quad (T_f - T_\infty)/(T_w - T_\infty) \tag{3}$$

and are parameterized by L_h/L, L_v/L and Ra.

RESULTS AND DISCUSSION

The presentation will begin with the Nusselt number results for the finned tube in free space (i.e. far from walls). These results provide the Q^* values which serve as the baseline in the Q/Q^* ratios for the finned tube in the presence of wall(s). The Q/Q^* ratios are presented next. The last set of results conveys temperature information at the fin tips, the sidewall and the floor.

Heat transfer in absence of walls

The Nusselt numbers Nu^* for the finned tube in free space are plotted in Fig. 3 as a function of the Rayleigh number, which serves as a dimensionless measure of the temperature difference $(T_w - T_\infty)$. To provide continuity, a smooth curve has been faired through the data. The observed increase of Nu^* with Ra is not unexpected, since both the convective and radiative contributions to Q^* increase more than linearly with $(T_w - T_\infty)$. As will be documented shortly, the relatively small numerical values of Nu^* do not mean that Q^* is small. A major factor in the magnitude of Nu^* is the use of the interfin spacing S (a relatively small quantity) as the characteristic dimension. Also, it is the quantity S^3 which causes the magnitude of Ra (ranging from about 40 to 1000) to appear small.

To obtain a practically useful measure of its magnitude, Q^* may be compared with the rate of heat transfer Q_{tube} from an unfinned horizontal tube whose diameter and length are the same as those of the finned tube. The comparison is made at common values of T_w, T_∞, ambient pressure, radiation surface properties, and with both the finned and unfinned tubes in free space. For an isothermal-walled, unfinned tube in free space, the convective and radiative heat transfer rates are additive, so that

$$Q_{tube} = [h_{tube}(T_w - T_\infty) + \varepsilon\sigma(T_w^4 - T_\infty^4)]A_{tube}. \tag{4}$$

The convective heat transfer coefficient for the unfinned tube was evaluated from a correlation based on the carefully conducted experiments of [3]

$$(hD/k)_{tube} = 0.592[\{g\beta(T_w - T_\infty)D_{tube}^3/\nu^2\}Pr]^{0.227}. \tag{5}$$

Each measured value of Q^* was ratioed with a corresponding value of Q_{tube} calculated from equations (4) and (5) ($D_{tube} = D = 3.188$ cm, $L_{tube} = 30.48$ cm, $A_{tube} = (\pi DL)_{tube}$, $\varepsilon = 0.87$). The thus-determined Q^*/Q_{tube} ratios are represented by the dashed line in Fig. 3. As seen there, Q^*/Q_{tube} is substantially greater than one, ranging from about 4 to 8 over the investigated range of Ra, i.e. of the temperature difference $(T_w - T_\infty)$. The departures of Q^*/Q_{tube} from one are indicative of the enhancements due to finning. The greatest enhancements occur in the range of large temperature differences, which is the range most relevant to practice. To provide perspective for the magnitude of the enhancement, it may be noted that the ratio of the surface areas of the finned and unfinned tubes is about 19.5.

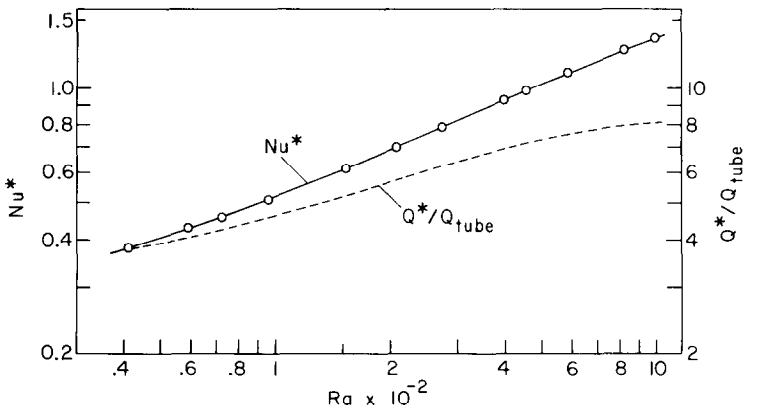

FIG. 3. Heat transfer results for the finned tube in free space.

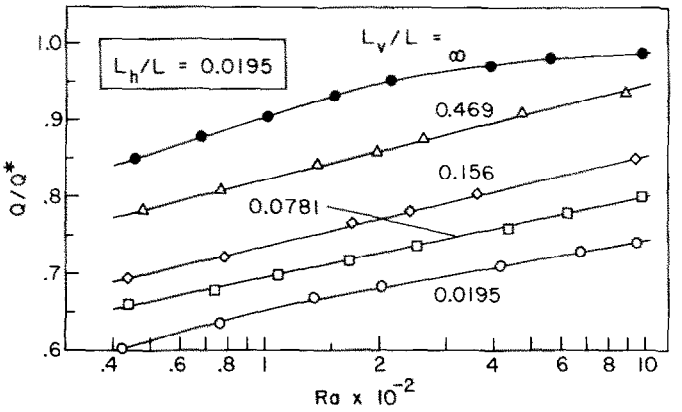

FIG. 4. Finned-tube heat transfer results in the presence of a sidewall/floor system, $L_h/L = 0.0195$.

Heat transfer in presence of walls

As noted earlier, the effect of a sidewall or of a sidewall/floor system on the finned-tube heat transfer will be conveyed by the ratio Q/Q^*, where Q is the heat transfer rate in the presence of the walls and Q^* is the heat transfer rate when there are no walls. This information is presented in Figs. 4–8, where Q/Q^* is plotted as a function of the Rayleigh number Ra for parametric values of the sidewall and floor clearance ratios L_h/L and L_v/L (L_h, L_v, and L are illustrated in Fig. 2). The results corresponding to sidewall/floor systems are set forth in Figs. 4–8(a), while those corresponding to the sidewall alone are plotted in Fig. 8(b). The latter case is inherently simpler than the former and will, therefore, be the starting point of the discussion.

In Fig. 8(b), the Q/Q^* vs Ra data are parameterized by seven values of the dimensionless clearance L_h/L between the fin tips and the sidewall ranging from 0.0195 to 0.938. This range encompasses both very small and very large clearances and spans the entire practical range. The absence of a floor is indicated by $L_v/L = \infty$. The respective data for $L_h/L = 0.0195$, 0.0781 and 0.156 are relatively distinct, and smooth curves have been faired through them for continuity. However, the data for the other cases are overlapping and, to avoid confusion, only one additional curve (that for the largest clearance $L_h/L = 0.938$) has been drawn.

An overview of Fig. 8(b) indicates that except for extreme conditions, the finned-tube heat transfer is not decisively affected by the presence of a sidewall, i.e. Q/Q^* does not differ appreciably from unity. The largest measured sidewall influence, $Q/Q^* = 0.85$, was encountered at the smallest values of Ra and L_h/L which, in operational terms, corresponded to $(T_w - T_\infty) \simeq 4°F$ and $L_h = 1/16$ in. Such small temperature differences and clearances are not highly likely in practice. For $Ra \geqslant 100$ ($\Delta T \geqslant 10°F$) and $L_h/L \geqslant 0.0781$ ($L_h \geqslant 0.25$ in.), the deviations of Q from Q^* are confined to the 3% range. The heat transfer corresponding to $L_h/L \geqslant 0.313$ ($L_h \geqslant 1$ in.) is virtually equal to Q^* for any Ra.

Although values of $Q < Q^*$ appear to be predominant in Fig. 8(b), it can be seen that in the range of moderate and larger Ra values and for $L_h/L \geqslant 0.0781$, Q/Q^* generally exceeds one. The possibility of such enhancement was noted in the Introduction. It may be attributed to the buoyancy imparted by the sidewall to the air, a buoyancy which is additional to that created by the finned tube itself.

Attention is now turned to the heat transfer results

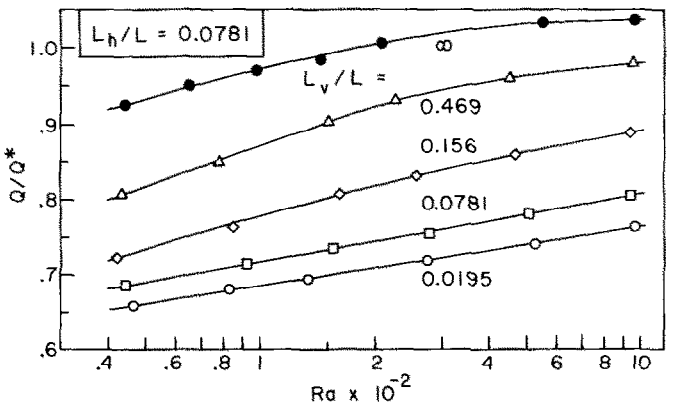

FIG. 5. Finned-tube heat transfer results in the presence of a sidewall/floor system, $L_h/L = 0.0781$.

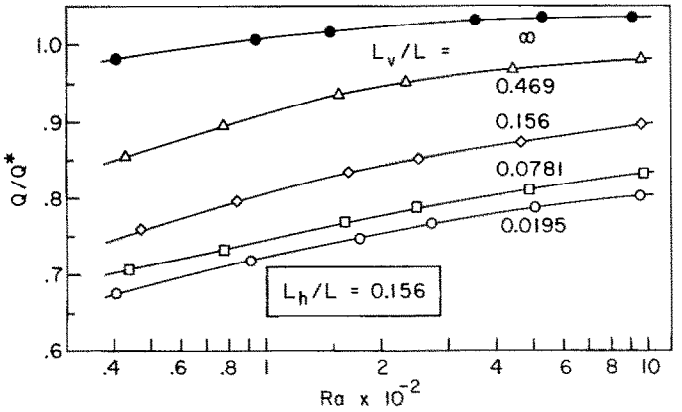

FIG. 6. Finned-tube heat transfer results in the presence of a sidewall/floor system, $L_h/L = 0.156$.

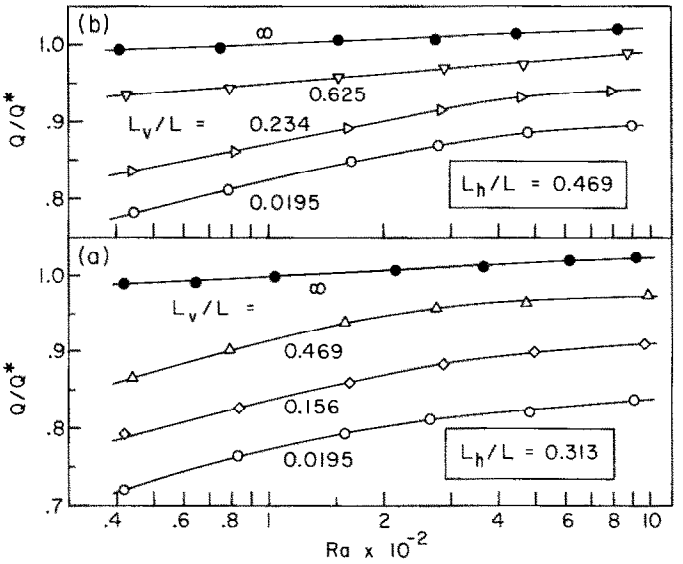

FIG. 7. Finned-tube heat transfer results in the presence of a sidewall/floor system, $L_h/L = 0.313$ and 0.469.

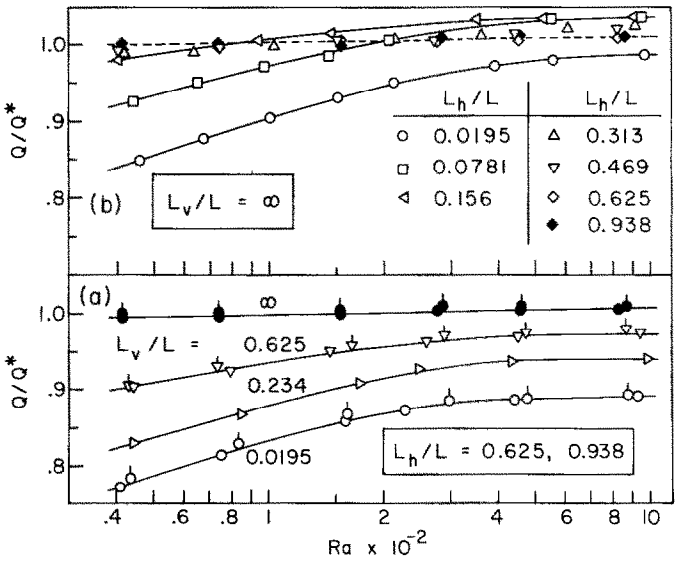

FIG. 8. Finned-tube heat transfer results in the presence of: (a) a sidewall/floor system with $L_h/L = 0.625$ and 0.938 and (b) a sidewall.

corresponding to the presence of a sidewall/floor system. Each of Figs. 4–8(a) conveys Q/Q^* vs Ra data for a fixed sidewall clearance L_h/L over a range of parametric values of the floor clearance L_v/L.

Figure 4 pertains to the smallest sidewall clearance $L_h/L = 0.0195$, with floor clearances L_v/L ranging from 0.0195 to ∞. The latter case (black data symbols) serves as a reference since it corresponds to the absence of the floor. It is evident from the figure that the presence of the floor results in a significant reduction in Q/Q^* compared to the no-floor case. Thus, the floor is a significant factor in the heat transfer process.

The lowest measured values of Q/Q^* occur at the smallest temperature differences and clearances. The reduction in Q relative to Q^* is seen to diminish as the floor clearance gap and the Rayleigh number increase. The lessening of the reduction in Q with increased floor clearance is altogether expected, but the Rayleigh number effect merits elaboration.

As already noted, the Rayleigh number serves as a dimensionless temperature difference. At small temperature differences, the percentage contribution of the radiative transfer to the convective–radiative heat loss is greater than at higher temperature differences (this can be easily verified for simple situations such as the unfinned horizontal tube, for which equations (4) and (5) apply). Consequently, if the radiative transfer is more severely affected by the presence of the walls than is the natural convection, Q/Q^* will be more reduced at lower Ra than at higher Ra.

Whereas Fig. 4 indicates the possibility of significant wall-related reductions in the finned-tube heat transfer, it should be noted that the figure corresponds to a very tight sidewall clearance (1/16 in.). The next figure, Fig. 5, pertains to a somewhat less tight clearance, namely, $L_h/L = 0.0781$ (0.25 in.). A quantitative comparison of Figs. 4 and 5 indicates a lessening of the reductons in Q with increasing L_h/L. However, the remaining reductions in Q are still by no means negligible. For example, in Fig. 5, for a floor clearance $L_v/L = 0.0781$ (0.25 in.), $Q/Q^* \sim 0.75$. All of the qualitative trends identified in Fig. 4 continue in force in Fig. 5.

A still larger sidewall clearance, $L_h/L = 0.156$ (0.5 in.) is considered in Fig. 6. Comparison of the Q/Q^* results of this figure with those of Fig. 5 confirm the further lessening of the reductions in Q. However, the lessening is gradual rather than precipitous, indicating the major role played by the floor relative to that of the sidewall. For the sidewall clearance of Fig. 6, it would appear acceptable to neglect the deviations of Q from Q^* only when $L_v/L \geqslant 0.469$ (1.5 in.), and only then for $Ra \geqslant 500$.

Figure 7 conveys results for both $L_h/L = 0.313$ and 0.469 (1 and 1.5 in.), respectively in the (a) and (b) parts of the figure. These values are on the outer fringe of the L_h/L that are encountered in practice. From this figure and from Fig. 6, it can be seen that whereas configurations with small floor clearances continue to respond to increases in the sidewall clearance, little response is in evidence when the floor clearance is large.

The independence of Q/Q^* from further changes in sidewall clearances becomes all pervasive in Fig. 8(a). This figure contains results for both $L_h/L = 0.625$ and 0.938 (2 and 3 in.) unflagged and flagged symbols, respectively). These sidewall clearances are larger than those of common practice. The virtual independence of Q/Q^* from L_h/L indicates that the floor now totally controls the deviations of Q from Q^*. For this situation and in the practical range of Ra and L_v/L, these deviations are not likely to exceed 5–10%.

Fin-tip temperatures

Representative fin-tip temperature data are presented in Fig. 9. These data convey the essential features of an extensive graphical presentation available in [2]. The dimensionless temperature ratio $(T_{tip} - T_\infty)/$

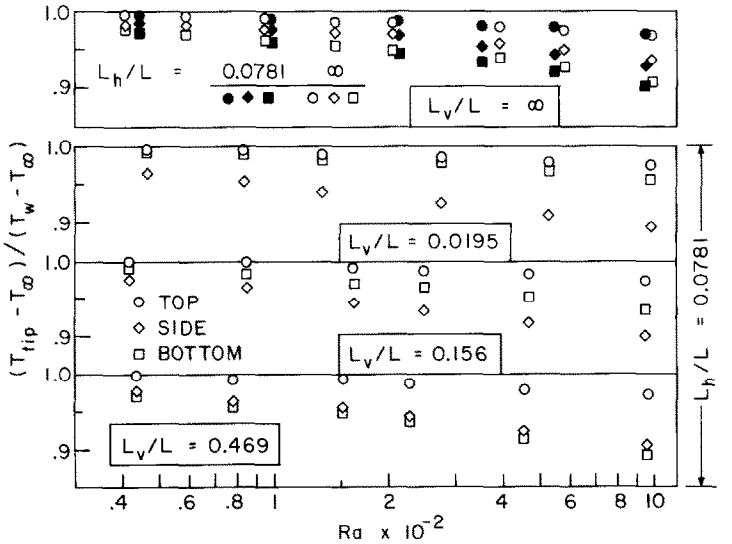

FIG. 9. Representative fin-tip temperatures.

$(T_w - T_\infty)$ used to display the results compares the tip-to-ambient temperature difference with the temperature difference between the tube wall and the ambient. For an isothermal fin (i.e. fin efficiency = 1), this temperature ratio is unity. Thus, the departure of the ratio from unity is a measure of the fin efficiency.

Figure 9 is subdivided into two parts. The single graph set apart from the others at the top of the figure corresponds to the no-floor case ($L_v/L = \infty$), while the other graphs correspond to the presence of a sidewall/floor system. In each graph, the dimensionless fin tip temperature is plotted as a function of the Rayleigh number. At each Rayleigh number, data are presented for the respective midpoints of the top, side and bottom edges of the fin. The side-edge temperature measurement was made at the side-edge which faces away from the sidewall (a thermocouple positioned at the sidewall-adjacent edge would, in all likelihood, not have survived at the tight clearances).

An overall examination of Fig. 9 reveals certain characteristics that are common to all cases. First, the values of $(T_{tip} - T_\infty)/(T_w - T_\infty)$ are, for the most part, in the range from 0.9 to 1, indicating that the fins were highly efficient for all of the operating conditions. Also, $(T_{tip} - T_\infty)/(T_w - T_\infty)$ drops off as the Rayleigh number increases, signaling a corresponding decrease in the fin efficiency. This dropoff with Rayleigh number indicates that the fin base-to-tip temperature difference $(T_w - T_{tip})$ increases more than linearly with $(T_w - T_\infty)$, which is consistent with the nonlinear dependence of the heat transfer rate on $(T_w - T_\infty)$, as discussed earlier.

The results presented for the no-floor case ($L_v/L = \infty$) correspond to two rather extreme sidewall clearances, $L_h/L = 0.0781$ (a very small clearance) and $L_h/L = \infty$ (no sidewall). The upper graph of Fig. 9 shows that the dimensionless fin-tip temperatures are virtually identical for the two sidewall clearances. It is also seen from the graph that the tip temperatures increase in an orderly manner from the bottom, to the side, to the top. This ordering reflects the temperature increase sustained by the airflow as it moves upward through the interfin spaces.

The tip temperature results corresponding to the sidewall/floor system are for a fixed sidewall clearance $L_h/L = 0.0781$ and for successively larger values of the floor clearance L_v/L (lower trio of graphs), culminating in the no-floor case (upper graph). The size of the floor clearance is seen to have a marked effect on the ordering of the tip temperatures. At the smallest floor clearance, the bottom-edge temperature is only slightly lower than the top-edge temperature, while the side-edge temperature is the lowest of the three. As L_v/L increases, the bottom-edge temperature decreases, finally dropping below the side-edge temperature. This behavior, which was encountered for all of the investigated geometries, is caused by the clearance-related restriction of the airflow in the neighborhood of the bottom edge of the fin. The severe restriction associated with very small clearances is relaxed as the clearance is increased, enabling the airflow to penetrate to the bottom edge and resulting in a decrease in the edge temperature.

Sidewall and floor temperatures

A representative sample of the measured sidewall temperature distributions (available in Figs. 5.18–5.23 of [2]) is presented in Fig. 10. On the ordinate, the sidewall-to-ambient temperature difference $(T_{sw} - T_\infty)$ is ratioed with the temperature difference $(T_w - T_\infty)$ between the tube wall and ambient. This ratio is plotted as a function of the coordinate Y which is measured vertically upward along the sidewall, with $Y = 0$ corresponding to the center of the finned tube as illustrated in the diagram at the lower left of the figure.

The figure consists of two graphs, respectively parameterized by $L_v/L = 0.0195$ and ∞ and corresponding to a tight floor clearance and to no floor. In each graph, data are plotted for two sidewall clearances—a tight clearance ($L_h/L = 0.0195$) and a clearance typical of practice ($L_h/L = 0.313$). Circles and squares are used to designate data at Ra values approximately equal to 40 and 1000, which correspond to the extremes of the investigated range.

As seen in the figure, the highest sidewall temperature for a given operating condition occurs just opposite the center of the tube (i.e. $Y = 0$). At that point, the rise of the sidewall temperature above ambient is 70–90% of the tube-wall temperature rise above ambient when the sidewall clearance is very small. The sidewall temperature tails off both in the directions above and below the tube, more slowly for the former than for the latter.

The sidewall temperatures diminish as the sidewall clearance increases. When the sidewall clearance is small, the presence or absence of a floor has virtually no effect. However, at larger sidewall clearances, the presence of a floor leads to higher temperatures. Furthermore, there is a tendency toward larger sidewall temperature rises, relative to $(T_w - T_\infty)$, at lower Rayleigh numbers.

Representative results for the floor temperature distribution are presented in Fig. 11, with a more

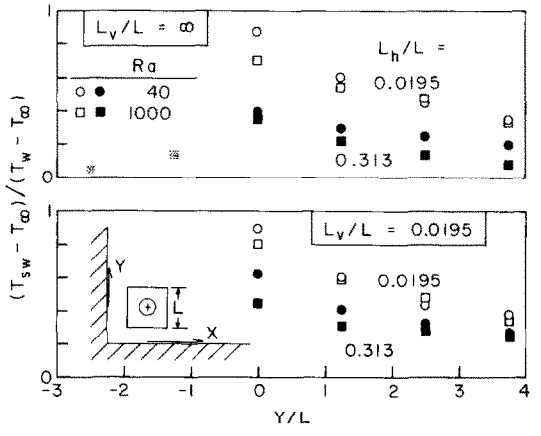

FIG. 10. Representative sidewall temperature distributions.

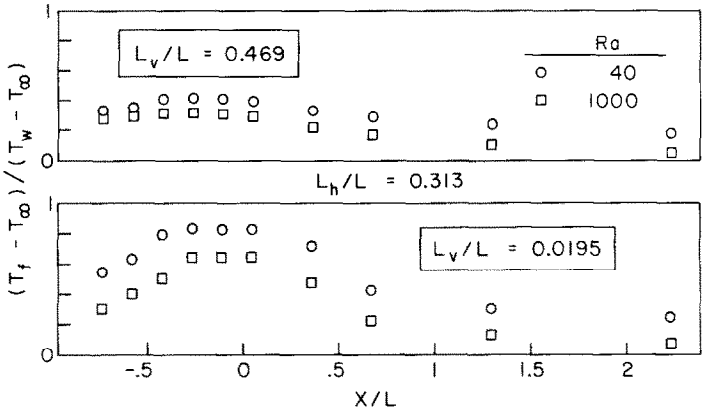

FIG. 11. Representative floor temperature distributions.

complete set of results available in Figs. 5.24–5.30 of [2]. On the ordinate, the floor temperature T_f is embedded in a dimensionless ratio analogous to that used in the presentation of the fin-tip and sidewall temperature results. The abscissa depicts the position coordinate along the floor, where X is defined in the inset of Fig. 10 (note that $X = 0$ corresponds to the center of the finned tube). Figure 11 conveys results for a sidewall clearance typical of practice ($L_h/L = 0.313$) and for two floor clearances ($L_v/L = 0.0195$ and 0.469).

Inspection of Fig. 11 shows that the temperature distribution along the floor displays a broad maximum whose breadth more or less subtends the side length L of the fins. The temperatures along the floor drop off with increasing distance from the finned tube, but less rapidly in the direction into the corner (i.e. negative X) than in the direction away from the corner. For the tightest floor clearance and the lowest Rayleigh number, the maximum attains a value ~ 0.8. The floor temperatures are responsive to changes in the floor clearance, decreasing as the clearance increases. At lower Rayleigh numbers, the temperature rise of the floor above ambient is a larger fraction of $(T_w - T_\infty)$ than at higher Rayleigh numbers.

CONCLUDING REMARKS

The experiments performed here have provided definitive results for the effects of a sidewall and of a sidewall/floor system on the convective–radiative heat transfer from a horizontal finned tube. Parametric variations, encompassing the practical range, were made for the clearances between the sidewall and the adjacent fin tips and between the floor and the adjacent tips. The temperature difference between the tube wall and the ambient, expressed in dimensionless terms via the Rayleigh number, was varied by a factor of 25.

The results presented in the paper are for the all-modes heat transfer, since it is this quantity that is needed in design. The generality of the results is enhanced by the fact that the radiation surface properties of the finned-tube apparatus and of the wall(s) (emissivities ~ 0.85) correspond to the practical realm of painted finned-tube heaters and nonmetallic floors and sidewalls. The low thermal conductivity of the walls used in the experiment is also characteristic of practice. As a further step toward generality, the heat transfer results are presented in the form of a ratio which tends to minimize the influence of the specific dimensions of the apparatus. The dimensions were chosen to conform to those commonly encountered in actual fin-tube heaters.

Three sets of experiments were performed: (1) finned tube in free space (i.e. far from walls), (2) finned tube in the presence of a sidewall, and (3) finned tube in the presence of a sidewall/floor system. The heat transfer results for the tube in free space were employed as a baseline against which the results for the tube in the presence of wall(s) were compared. In their own right, the results for the free-space case displayed 4-fold to 8-fold enhancements, depending on the temperature difference, relative to the heat transfer from a corresponding unfinned tube.

The presence of a sidewall had only a moderate effect on the finned-tube heat transfer. Although reductions as large as 15% were encountered over the investigated range of parameters, the sidewall effect is on the order of 5% in the practical range. For certain conditions, the presence of the sidewall may actually increase the finned-tube heat transfer by a few percent relative to the free-space case.

The presence of a sidewall/floor system brings about larger deviations from the no-walls case—always reductions. Wall-related reductions in finned-tube heat transfer of up to 40% were measured, but reductions in the 10–20% range are realistic for practical operating conditions.

The effect of the presence of the wall(s) was found to diminish with increases in the temperature difference between the tube and ambient. As expected, the effect of the walls was heightened as the wall-to-fin clearances decreased.

To supplement the heat transfer results, measurements were made of the fin-tip temperatures and of the

temperature distributions along the sidewall and the floor.

REFERENCES

1. R. R. Laschober and G. R. Sward, Correlation of the heat output of unenclosed single and multiple-tier finned-tube units, *Trans. Am. Soc. Heat. Air Condit. Eng.* **73**, 1–15 (1967).
2. M. A. Ansari, Natural convection and radiation from a finned horizontal tube with vertical and horizontal shrouding surfaces, Thesis, Department of Mechnical Engineering, University of Minnesota, Minneapolis, Minnesota, 1983.
3. D. C. Boessneck, Effect of transverse misalignment on natural convection heat transfer from a pair of horizontal parallel cylinders, Thesis, Department of Mechanical Engineering, University of Minnesota, Minneapolis, Minnesota, 1981.

TRANSFERT THERMIQUE CONVECTIF–RADIATIF A PARTIR D'UNE TUBE AILETE HORIZONTAL AVEC DES INTERACTIONS DE PAROI LATERALE OU PAROI LATERALE-PLANCHER

Résumé—On conduit des expériences pour déterminer le transfert thermique à partir d'un tube aileté horizontal répond à la présence d'une paroi latérale ou d'un système paroi latérale/plancher. On fait varier l'espace entre les sommets des ailettes et la paroi latérale et entre les sommets des ailettes et le plancher et, pour chaque configuration, les transferts thermiques sont obtenus pour un domaine de 25 essais de différence de température entre tube et ambience. Des mesures sont aussi faites pour le tube aileté situé dans un espace libre (c'est-à-dire loin de toute paroi) et ces résultats montrent un transfert thermique fortement augmenté (d'un facteur entre 4 et 8 fois) par rapport au cas d'un tube correspondant non aileté. La présence d'une paroi latérale a un effet modéré sur le transfert d'un tube aileté, alors que le système paroi latérale/plancher cause des changements plus importants. La réduction extrême dans ce dernier cas est d'environ 40%, mais des réductions de 10–20% sont plus réalistes pour des conditions pratiques. Relativement, la présence de paroi (s) a un moindre effet pour les grandes différences de température que pour les petites. On présente aussi des mesures de température au sommet des ailettes du coté de la paroi et du plancher.

WÄRMEÜBERGANG DURCH KONVEKTION UND STRAHLUNG VON EINEM HORIZONTALEN RIPPENROHR

Zusammenfassung—Es wurden Experimente durchgeführt, um den Einfluß einer Seitenwand oder einer Seitenwand und eines Bodens auf den Wärmeübergang an einem horizontalen Rippenrohr zu bestimmen. Als Parameter wurde der Abstand zwischen Rippenende und Seitenwand sowie zwischen Rippenende und Boden variiert. Es wurden auch Messungen mit Rippenrohren im freien Raum (weit entfernt von Wänden) durchgeführt. Diese Versuche zeigen einen wesentlich höheren Wärmeübergang (4–8 mal höher) im Vergleich zu einem entsprechenden, nicht berippten Rohr. Die Seitenwand hat nur einen mäßigen Einfluß auf den Wärmeübergang am Rippenrohr, während das System aus Seitenwand und Boden größere Änderungen bewirkt. Beim letzteren System betrug die größte Verringerung des Wärmeübergangs 40%, bei der praktischen Anwendung sind Verringerungen im Bereich von 10–20% realistischer. Bei großen Temperaturdifferenzen ist der Einfluß der Wand (Wände) prozentual geringer als bei kleinen Temperaturdifferenzen. Temperaturmessungen am Rippenende, an der Seitenwand und am Boden wurden ebenfalls durchgeführt.

ВЛИЯНИЕ БОКОВОЙ И НИЖНЕЙ СТЕНОК НА КОНВЕКТИВНО-РАДИАЦИОННЫЙ ПЕРЕНОС ОТ ГОРИЗОНТАЛЬНОЙ ОРЕБРЕННОЙ ТРУБЫ

Аннотация—Выполнены экспериментальные исследования по определению влияния бокового или нижнего расположения стенки на теплообмен горизонтальной оребренной трубы. В процессе опытов менялось расстояние между вершинами ребер и различным образом расположенной стенкой и для каждого сочетания исследовались характеристики теплообмена при 25-кратном уровне разности температур между поверхностью трубы и окружающей средой. Измерения оребренной трубы, помещенной в свободное пространство (т.е. вдали от стенок) показали возрастание теплообмена (в 4–8 раз) по сравнению с соответствующей неоребренной трубой. Наличие боковой стенки оказывает умеренное влияние на теплообмен оребренной трубы, в то время как нижняя стенка вызывает значительные изменения. Наибольшее уменьшение теплопереноса в последнем случае составило около 40%, в обычных рабочих условиях более реален уровень снижения на 10–20%. В процентном отношении пристутствие стенки(нок) оказывает меньшее действие при больших разностях температур. Представлены измерения температур на вершинах ребер, боковой и нижней стенках.